Battery performance enhancement with additions of bismuth

J.E. Manders
Pasminco Limited, P.O. Box 1291K, Melbourne, Vic. 3001 (Australia)

L.T. Lam*, R. De Marco, J.D. Douglas, R. Pillig and D.A.J. Rand
CSIRO, Division of Mineral Products, P.O. Box 124, Port Melbourne, Vic. 3207 (Australia)

Abstract

Automotive and valve-regulated batteries (VRBs) of typical commercial design have been constructed using positive and negative plates produced from leady oxide that is doped with 0.06 wt.% bismuth. The doping is performed by adding bismuth (III) oxide powder during the paste-mixing stage. Both battery designs have been subjected to endurance tests (automotive batteries: JIS cycle-life test; VRBs: repetitive 3-h discharge) in parallel with batteries that are similar in all respects but do not contain bismuth. A strategy and necessary hardware have been developed to measure the gassing properties of the VRBs during both charge and discharge. The procedure involves monitoring the internal pressure with high-precision pressure transducers. For automotive batteries, doping with bismuth produces no significant differences in JIS cycle life. By contrast, both the endurance and the capacity of VRBs are found to be enhanced by the presence of bismuth. Furthermore, bismuth reduces the build-up in gas pressure (mainly oxygen) in VRBs during constant-current charging. These results suggest that future specifications for leady oxide should include a minimum – rather than a maximum – bismuth content. In this respect, although studies performed to date show that significant advantages can be achieved with 0.06 wt.% bismuth in the active material, the optimum bismuth level has yet to be established.

Research objective

Valve-regulated batteries (VRBs) using absorbent glass-mat separators have been developed for a wide range of industrial and consumer applications. Ideally suited to stand-by energy storage, the technology is capturing increasing shares of both the telecommunications and the uninterruptible power-supply (UPS) markets, that is, in applications where only relatively shallow discharges or low numbers of charge/discharge cycles are required. Although VRBs are not, at present, used for the starting, lighting and ignition of automobiles, several manufacturers have batteries under development for just such a purpose.

The recombination of gases in this type of VRB relies heavily on both the structure and the degree of acid saturation of the glass-mat separator that is used to immobilize the electrolyte. In addition, it is of the utmost importance to minimize gas generation and to facilitate oxygen reduction (recombination) at the negative plates. To restrict gassing to manageable rates, battery manufacturers select starting materials of specific

*Author to whom correspondence should be addressed.

0378-7753/94/$07.00
SSDI 0378-7753(93)01861-B

quality for the manufacture of VRB designs. In particular, primary lead of high purity is generally specified as the raw material for oxide production. Lead–calcium–tin alloys are employed for grid fabrication in preference to antimonial types because of the latter's depolarizing effect on the hydrogen overvoltage at the negative plate. The removal of antimony, however, limits the ability of the positive plates to provide reliable and adequate service under deep-cycling duties. As a consequence, considerable research is being directed towards enhancing the cycling capability of antimony-free systems.

A collaborative research project between Pasminco Limited and CSIRO Division of Mineral Products commenced in 1989 with the objective to improve the deep-discharge performance of low-maintenance, flooded-electrolyte batteries. The approach has been to treat the positive and negative plates of these batteries with different dopants. The doping studies began with examining the effect of adding tin, selenium, bismuth, indium or germanium oxides. Early results showed that the most promising dopants were tin, selenium and bismuth.

In view of the growing demand for VRBs, the objective of the Pasminco/CSIRO project has been modified. Specifically, the experimental programme has been redirected towards the successive determination of the influence of different dopants, both singularly and collectively, on the gassing characteristics, capacity and cycle life of VRBs. (Note, it is important to confirm that any advantage in battery performance gained by using a given dopant is not offset by a concomitant increase in the gassing rate, especially at the negative plate.) As with the previous work, the new research strategy commenced with the doping of positive and negative active materials with each minor element in the oxide form. Since dopants are leached more readily into solution from the active material than from the grid, this procedure will yield a more rapid indication of any adverse action of the chosen dopant on the gassing behaviour at the negative plate. Following on from this exploratory work, a programme is now in place to assess the effects of incorporating the most promising of the minor elements in the grid alloy itself. The work reported here examines the influence of bismuth, added to the active materials, on the performance of both flooded-electrolyte and VRBs.

Experimental programme

Construction of automotive batteries

Positive and negative plates were prepared according to the paste formulae given in Table 1. The pastes were applied to standard, automotive, lead–antimony grids that contained ~1.7 wt.% antimony, tin, and common grain-refiners. Bismuth-doped plates were produced by adding bismuth(III) oxide powder to 'bismuth-free', Barton-pot oxide at levels of 0.015, 0.03 and 0.06 wt.% Bi. Plate curing was performed under 50 °C / high r.h. conditions for 24 h, followed by drying for a further 24 h. The cured plates were then assembled into NS40 type, 12-V, automotive batteries (four positive and five negative plates per cell) at a local battery-manufacturing plant. The batteries were filled with 1.07 sp. gr. H_2SO_4 and then subjected to container formation at a current of 5 A for 20 h.

During battery assembly, the plates were chosen so that repeat cells had, as closely as possible, the same total positive active mass and the same total negative active mass. Note, this design feature was also adopted in the construction of the VRBs discussed in the next section.

TABLE 1

Paste formulae for automotive batteries

Component	Positive electrode	Negative electrode
Leady oxide (kg)	3	3
Fibre (g)	1.5	1.8
Stearic acid (g)		1.8
$BaSO_4$ (g)		11.1
Vanisperse (g)		11.1
Carbon black (g)		6.3
1.40 sp. gr. H_2SO_4 (cm^3)	280	240
Water (cm^3)	400	380
Acid-to-oxide ratio (%)	6.5	5.6
Paste density (g cm^{-3})	4.2–4.3	4.3–4.4

TABLE 2

Paste formulae for valve-regulated batteries

Component	Positive electrode	Negative electrode
Leady oxide (kg)	3	3
Fibre (g)	0.9	1.8
CMC[a] (g)	7.5	
Stearic acid (g)		1.8
$BaSO_4$ (g)		11.1
Vanisperse (g)		11.1
Carbon black (g)		6.3
1.40 sp. gr. H_2SO_4 (cm^3)	200	200
Water (cm^3)	390	330
Acid-to-oxide ratio (%)	4.7	4.7
Paste density (g cm^{-3})	4.5–4.6	4.7–4.8

[a]Carboxymethyl cellulose.

Construction of valve-regulated batteries

Positive and negative plates were prepared using the paste formulae given in Table 2. Both polarities of plate were doped with 0.06 wt.% Bi. The grids were cast from Pb–0.09wt.%Ca–0.4wt.%Sn alloy. Plate curing was conducted at 50 °C / high r.h. for 24 h, followed by drying for an additional 72 h. Five positives and six negatives per tub were tank-formed at a constant current of 25 A for 6 h, and then rested at open circuit for 1 h. This charge/rest procedure was repeated and then followed by a final 6 h of charging. After formation, the plates were sent to a local battery-manufacturing facility for assembly. Each cell consisted of four positive and five negative plates. (Note, experiments were conducted on single 2-V valve-regulated cells, but for ease of expression, these are referred to here as valve-regulated batteries (VRBs).)

Cycle-life evaluation of automotive batteries

The Japanese Industrial Standard (JIS) endurance cycling regime was selected to assess the performance of the automotive batteries. The batteries were maintained

at 40±1 °C in a thermostatically-controlled water bath. Discharge was conducted at 10 A for 1 h, and recharge at 2.5 A for 5 h. This charge/discharge schedule is referred to as '1 cycle'. Following each 25 cycles, the batteries were discharged at 10 A until the terminal voltage decreased to 10.2 V. At this stage, the discharge time was recorded. The batteries were fully charged prior to the commencement of the next period of 25 cycles. The procedure was repeated until the capacity fell to 50%, or less, of the nominal 5-h rate capacity (27.6±0.8 Ah).

Cycle-life evaluation of valve-regulated batteries

The cycle-life performance of the VRBs was determined by using a repetitive 3-h discharge duty. After discharge to 1.7 V at 22.5 A (i.e., 3-h rate), the batteries were recharged at 15 A to a top-of-charge voltage of 2.45 V for approximately 3 h, and then held at a constant voltage of 2.45 V for a further 21 h. The procedure was repeated until the measured capacity was equal to 80% of the nominal value (67.5 Ah).

Gassing measurements on pasted electrodes

The design of the pasted electrode is shown schematically in Fig. 1. A section of a Pb–0.09wt.%Ca–0.4wt.%Sn grid (i.e., the type used in the construction of the VRBs) was embedded in epoxy resin to give a cylindrical mould. The unsoldered end of the grid was allowed to protrude about 2 mm above the upper surface of the mould (Fig. 1(a)). A polyvinyl chloride (PVC) rod with the same diameter as the assembly was sectioned into slices of thickness = 3 mm. A hole (diameter = 6 mm) was drilled through the centre of each slice and a cylindrical paper strip was fixed to the wall of the hole. The PVC slice was placed on the upper surface of the electrode assembly so that the grid was located at the centre of the hole (Fig. 1(a)). Untreated and doped pastes were prepared using the formulae given in Table 2. For doped material, the given element was added as an oxide powder to the leady oxide at a level of 0.1 wt.%. The resulting mixture was shaken in a container for 5 min prior to paste-mixing. The hole in the above assembly was filled with paste and the PVC slice was then removed to give the final dimensions of the electrode, as shown in Fig. 1(b).

The pasted samples were cured to tribasic lead sulfate ($3PbO \cdot PbSO_4 \cdot H_2O = 3BS$). After curing, the samples were placed in a petri disk that contained 1.07 sp. gr. H_2SO_4. Electrode formation was achieved by applying, for 20 h, a constant current of 17.7 mA per g of cured material.

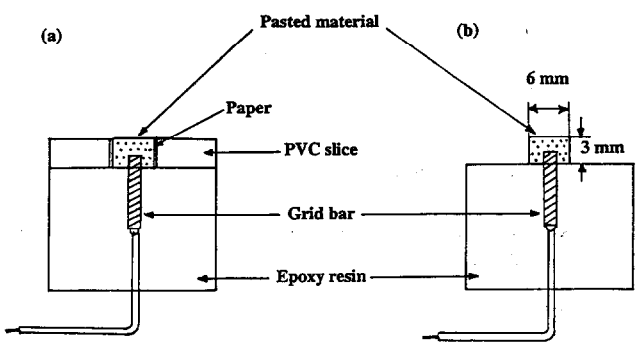

Fig. 1. Preparation of pasted electrodes for electrochemical studies.

The electrochemical cell used for gassing measurements is presented schematically in Fig. 2. The Pyrex cell has an H-shape; the two main compartments are separated by a glass frit. The electrolyte (1.275 sp. gr. H_2SO_4) was de-gassed with nitrogen for 30 min before introduction into the cell. The working electrode was the sample of plate material, as prepared above. A sheet of pure lead served as the counter electrode. All potentials were measured (and are reported) with respect to a 5 M Hg/Hg_2SO_4 reference electrode in 1.275 sp. gr. H_2SO_4.

The potential of the working electrode was scanned either between -1.1 and -1.7 V or between 1.3 and 1.7 V at 5 mV s^{-1} for 20 cycles prior to measurement of the hydrogen or oxygen rates, respectively. Over these two potential ranges, any lead sulfate residues (resulting from incomplete formation and/or the chemical development of sulfation layers) will be converted, respectively, to lead or lead dioxide. A potential-step technique, together with gas collection, was used for studies of both hydrogen and oxygen evolution. The procedure involved stepping the potential of the sample to a given value and then holding for a given period. During this time, the potential, the total delivered current and the quantity of charge were recorded.

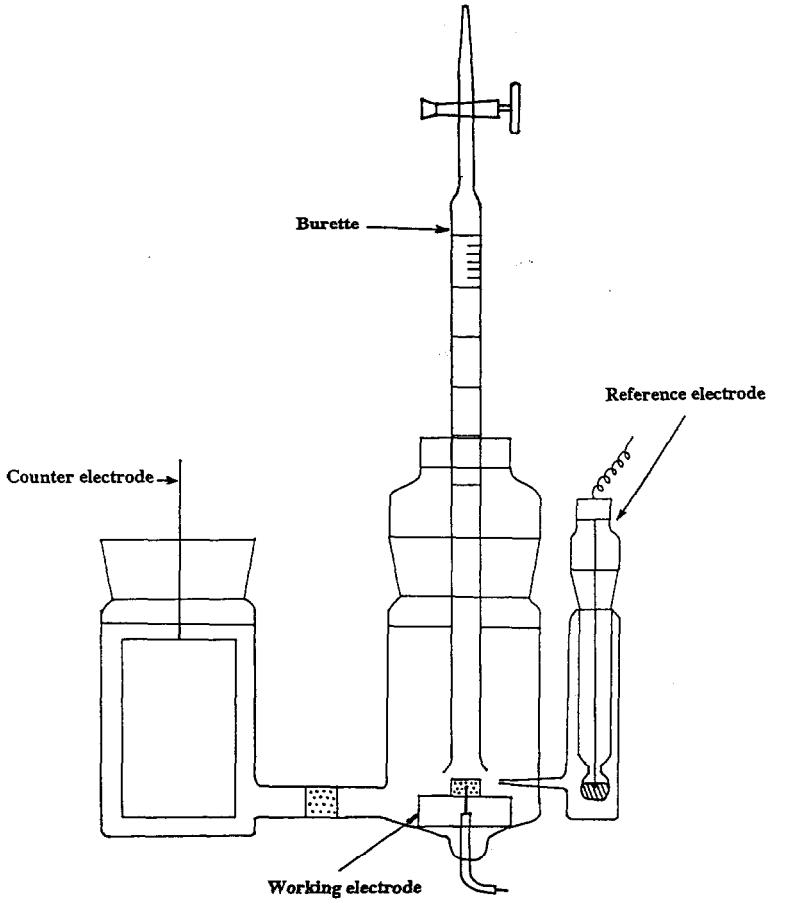

Fig. 2. Electrochemical cell used for gassing measurements.

Simultaneously, the gas produced was collected by solution displacement in a 25 ml burette that was located immediately above the sample. The hydrogen- or oxygen-evolution current density at different potentials was calculated from the corresponding amount of gas collected [1].

Gassing measurements on valve-regulated batteries

Commercial pressure transducers (Keller Series 9, PR-9-0.5) were used to monitor the internal pressure of the VRBs. The specifications of these devices are:

- linear response over a full scale of 60 kPa in the temperature range −10 to 80 °C
- reproducibility of pressure measurements: <0.15% (for full scale)
- sensitivity: ±0.01 kPa

A hole of 1.5 cm diameter was drilled into the lid of the container. A pressure transducer was attached to each battery using a specially-designed perspex receptacle that covered the hole and was glued to the lid of the container. This design provided a gas-tight seal between the receptacle and an O-ring that surrounded the transducer. It also served to fix the transducer rigidly in position. The transducers were driven by electronic units that were designed and built in the CSIRO laboratories. Before attachment to the cells, the transducers were calibrated against a mercury manometer; a linear relationship was achieved between the response of the transducer and the gas pressure (Fig. 3). Commercial pressure-relief valves were also attached to the batteries. These were set to vent at about 21 kPa. Current, voltage and pressure were recorded on an IBM computer. The data-acquisition system utilized a 'Workbench' software package.

Determination of oxygen-recombination efficiency in VRBs

During the overcharging of VRBs at constant current, the principal reactions are the evolution of oxygen at the positive plate, and the reduction of lead sulfate (formed as a result of the recombination of oxygen) together with the evolution of hydrogen

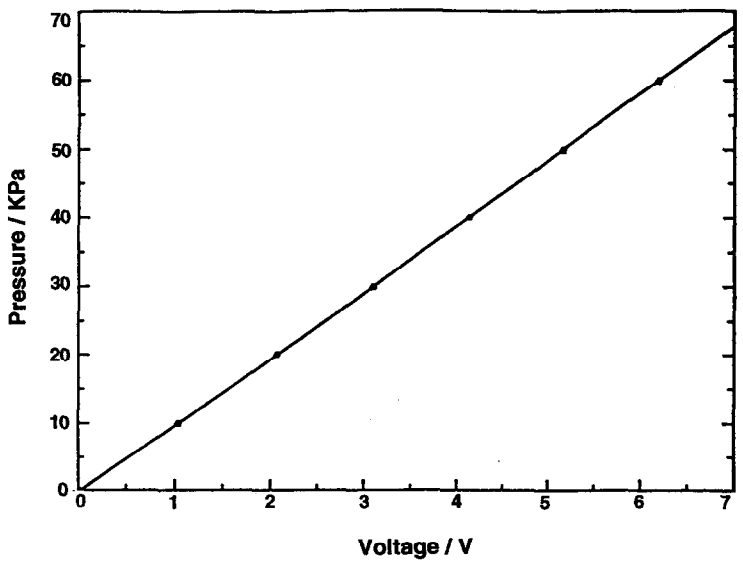

Fig. 3. Calibration graph for pressure transducer.

at the negative plate. All other reactions, such as positive grid corrosion and oxidation of organic compounds are negligible (see Figs. 9 and 10, later). Therefore, the measurement of the cell overpressure during galvanostatic overcharge and after circuit interruption can be used to determine the oxygen-recombination efficiency [2–5]. Using this procedure, the ratio between the oxygen-recombination current and the overcharge current is taken as a measurement of the oxygen-recombination efficiency, provided that the battery is fully charged prior to each test.

Results

Chemical composition of the cured plates

Two automotive batteries were prepared for each concentration of bismuth (i.e., 0, 0.015, 0.03 and 0.06 wt.% Bi). The crystalline phase composition of the cured positive and negative plates is presented in Fig. 4(a) and 4(b), respectively. It can be seen that the concentrations of monobasic lead sulfate (1BS) and β-PbO in the positive plates are similar to those in the negatives. Although 1BS is known to degrade the strength of formed plates, the observed content ($\sim$5 wt.%) is insufficient to affect adversely the plate performance. The formation of the high-temperature polymorph of PbO (i.e., β-PbO) is difficult to explain. It should be pointed, however, that Pavlov and Papazov [6] have also observed the development of β-PbO during paste mixing. A greater content of tribasic lead sulfate (3BS) was detected in the cured positives; this was due to the higher acid-to-oxide ratio of the positive-paste formula (see Table 1).

Five valve-regulated batteries were constructed for each bismuth level (viz., 0 and 0.06 wt.% Bi). The crystalline phase composition of the cured positive and negative plates is given in Fig. 5(a) and (b), respectively. In contrast to the results obtained for automotive plates, the positives and negatives are similar in all aspects of phase composition (note, the error of the XRD technique is about $\pm$4 wt.%). This is due to the fact that an identical acid-to-oxide ratio was used in both the positive and negative paste formulae (see Table 2).

The data for different paste runs (Figs. 4 and 5) indicate that there is good plate-to-plate consistency between the phase composition of the cured materials in the above two battery designs. An equally significant observation is that the addition of bismuth, at the levels used to date, does not produce any noticeable changes in the relative abundances of the component phases. Thus, any subsequent effects on battery performance are likely to arise from the action of bismuth itself rather than from secondary modification of the phase chemistry of the cured plates.

JIS endurance cycling

The average number of cycles (mean value for two batteries) at which the bismuth-doped and untreated automotive batteries failed under JIS cycling are presented in Fig. 6. Since a difference in performance of less than 25 cycles reflects an insignificant variation in the JIS endurance, it is clear that bismuth exerts only a slight beneficial effect. Autopsies revealed that the major modes of failure were associated both with excessive shedding of positive active material and with heavy grid corrosion. Furthermore, it was found that bismuth, in either the positive or negative plate, does not dissolve into the electrolyte during charge/discharge cycling [7].

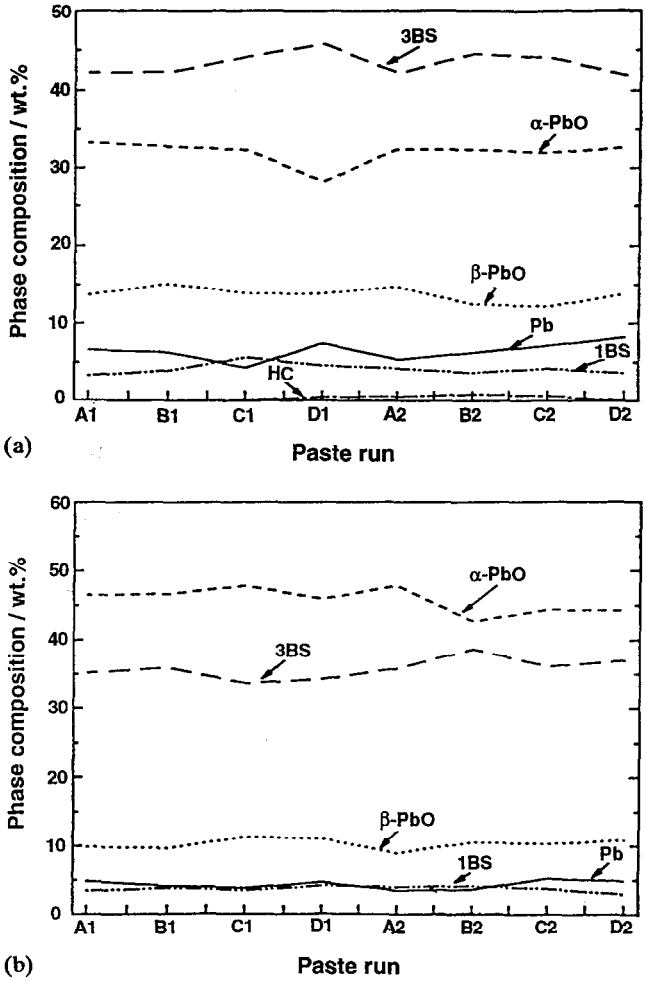

Fig. 4. Phase distribution in cured automotive battery plates: (a) positive; (b) negative. Letters A, B, C and D correspond to batteries containing 0, 0.015, 0.03 and 0.06 wt.% Bi, respectively. The accompanying number 1 and 2 signifies the paste run. (Note, only trace amounts of $2PbCO_3 \cdot Pb(OH)_2$=HC were found in the negative plates).

Repetitive 3-h discharge cycling

Figure 7 shows the number of cycles that were completed before failure by VRBs that used either bismuth-doped or untreated positive and negative plates. The results clearly demonstrate that significant increases in cycle life are obtained with the addition of 0.06 wt.% Bi. (Note, further investigations are in progress to seek an explanation for the marked difference in the enhanced performance that was given by the two batteries (D_1, D_2) under test.) Moreover, the capacity of the bismuth-doped batteries was found to be consistently higher than the untreated counterparts throughout the period of cycling duty. In general, an 8% improvement in capacity was observed.

The total energy output (kWh) from both the bismuth-doped and the untreated batteries during the cycling programme is shown in Fig. 8. For bismuth-doped batteries

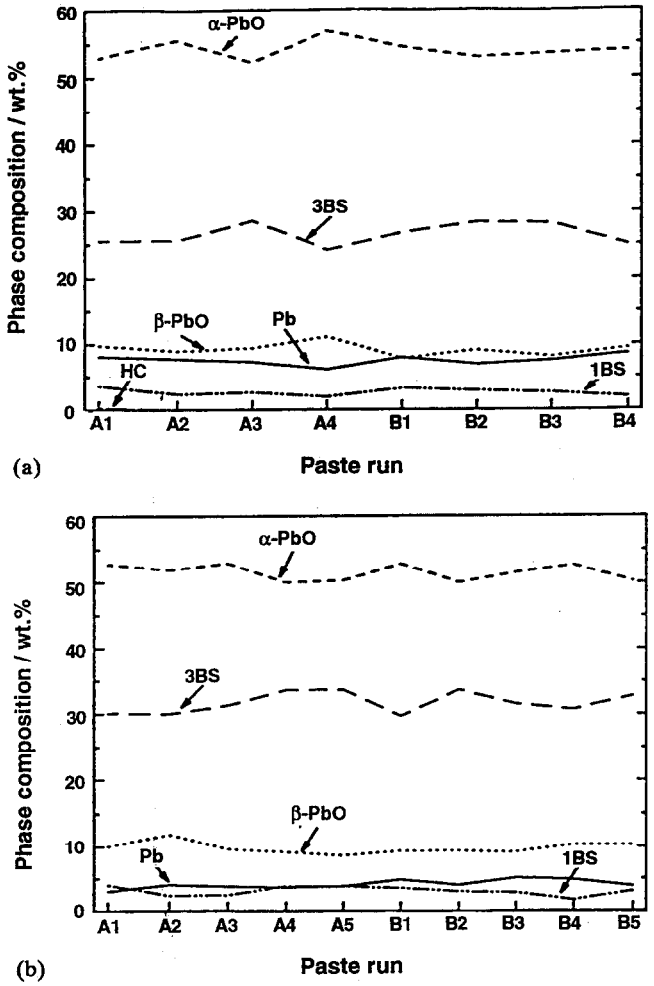

Fig. 5. Phase distribution in cured valve-regulated battery plates: (a) positive; (b) negative. Letters A and B correspond to batteries containing 0 and 0.06 wt.% Bi, respectively. The accompanying number 1 to 5 signifies the paste run.

the combination of higher capacity and longer cycle life (see above) results in a large increase in the energy output. In cycling applications of lead/acid batteries (e.g., motive power, solar energy storage, load-levelling), the total work performed (i.e., the energy output) over the life of a battery is a more meaningful assessment of battery performance since equivalent numbers of charge/discharge cycles for different batteries may represent differing amounts of work performed by these batteries.

Gassing behaviour of pasted electrodes

Hydrogen-evolution rates and efficiencies for both bismuth-doped and untreated negative samples are given in Fig. 9. (Note, two or more separate determinations of the gassing rate were undertaken at each potential. The average values are reported here.) The hydrogen-evolution rate on the bismuth-doped sample is higher than that

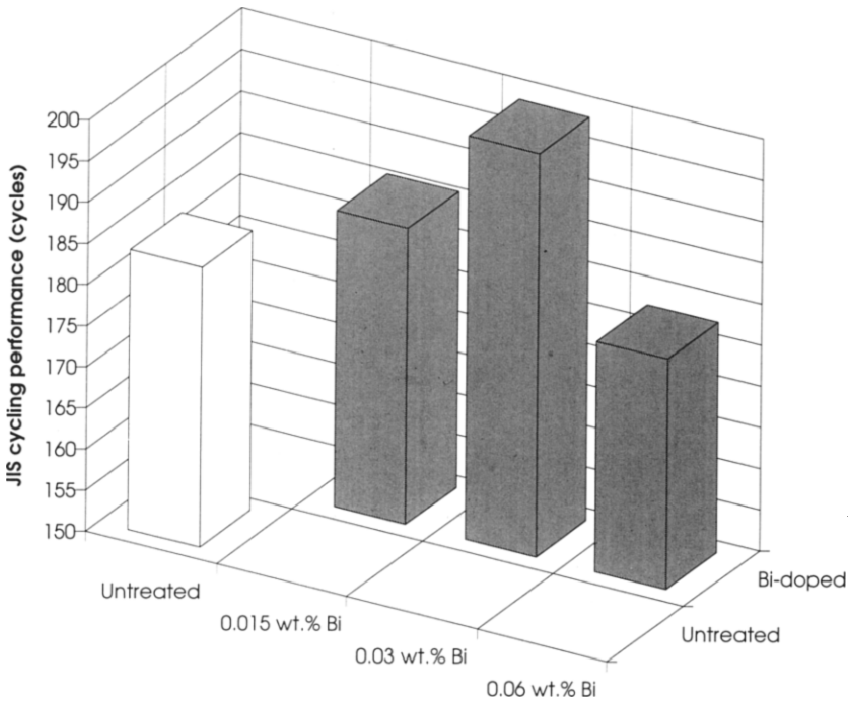

Fig. 6. Life-cycle performance of automotive batteries under JIS conditions.

on the untreated counterpart, especially at potentials that are more negative than −1.5 V. The initial hydrogen-evolution efficiency for both the bismuth-doped and untreated samples is high (viz., ~94% at −1.4 V) and increases rapidly to ~98% at −1.5 V and thereafter. This indicates that the accuracy of the procedure used for measurement of this parameter is ~2%; the small error is caused by the tenacious attachment of some gas bubbles to the wall of the burette.

The oxygen-evolution rate at different potentials is presented in Fig. 10. Again, the bismuth-doped electrode exhibits the higher gassing rate. Moreover, the difference between the rates of oxygen evolution on the bismuth-doped and untreated electrodes is larger than that observed between the corresponding rates of hydrogen gassing. The efficiency of oxygen evolution on the fully-formed electrodes is ~96%. Given the above-mentioned accuracy of the gas-collection technique, this value of the efficiency indicates that, during overcharge, most of the current goes into gassing; the remainder is associated with corrosion of the grid and other possible oxidation processes.

Gassing behaviour of valve-regulated batteries

The pressure peaks developed in bismuth-doped and untreated VRBs during the constant-current charging period at advancing stages of cycling are listed in Table 3. Although the data are scattered, the overall trend reveals that the pressure peaks are lower in the case of the bismuth-doped batteries. It has been reported [8, 9] that the oxygen-reduction process in sulfuric acid solution is purely a chemical reaction that is both independent of the negative-plate potential and increases with increasing oxygen solubility. In the valve-regulated system, this reduction rate is proportional to the oxygen partial-pressure, as well as to the effective surface area of the negative plate.

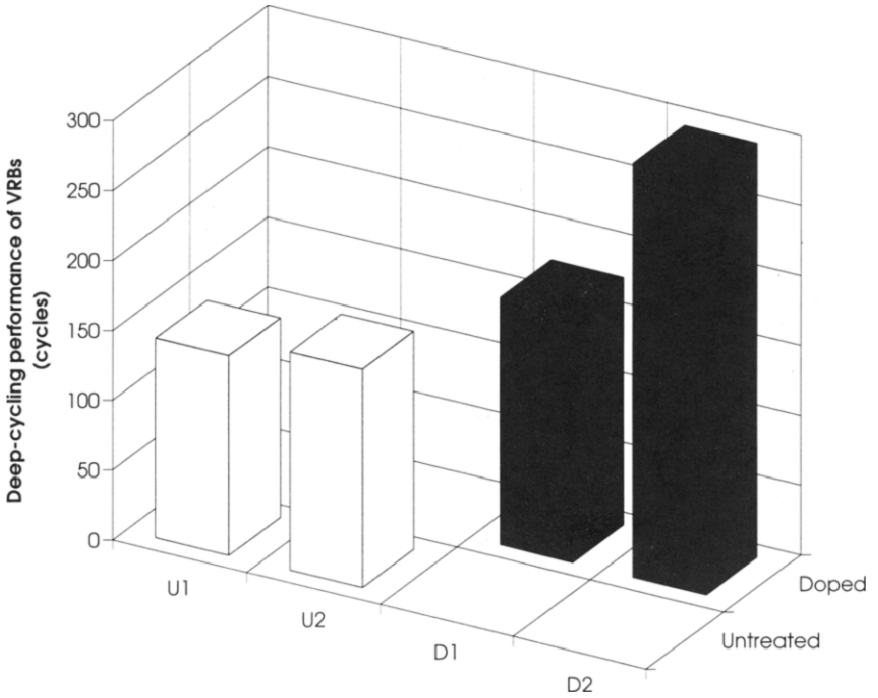

Fig. 7. Life-cycle performance of valve-regulated batteries under repetitive 3-h discharge conditions. U1, U2 = untreated batteries; D1, D2 = batteries with 0.06 wt.% Bi.

On the other hand, the rate is disproportional to the thickness of the electrolyte layer at the negative plate [2–5]. In addition, it has been confirmed above that the oxygen-evolution rate on bismuth-doped electrodes is higher than that on untreated electrodes (see Fig. 10). Thus, in the case of batteries, the oxygen-reduction rate during constant-current charging should be higher for cells using bismuth-doped positive plates than for untreated equivalents because of the higher oxygen partial-pressure. Furthermore, Maja and Penazzi [10] have shown that the presence of bismuth in the negative active material facilitates the rate of oxygen reduction. With bismuth-doped batteries, therefore, both of these advantageous factors will serve to restrict the build-up in pressure due to the progressive accumulation of any uncombined oxygen.

Table 4 shows the oxygen-recombination efficiency determined at intervals of 20 cycles. Reasonably stable values of around 90% were obtained. There was little difference between the oxygen-recombination efficiencies of the bismuth-doped and the untreated batteries.

Discussion

Debate over the effects of bismuth on battery performance has persisted for many years within both the battery and the lead industries. Unfortunately, although numerous investigations have been conducted, very little of the work has been performed on practical battery systems. Furthermore, there have been no studies at all on valve-regulated technology. To provide a comparison with the investigations reported here, a survey is given below of the limited literature that concerns the influence of bismuth

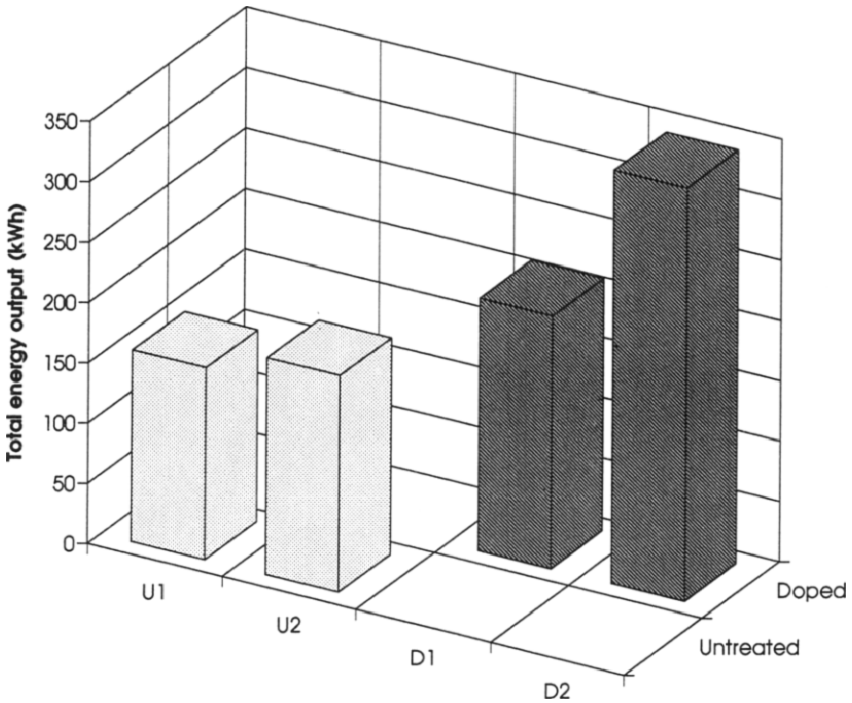

Fig. 8. Cumulative energy output of valve-regulated batteries under repetitive 3-h discharge conditions. U1, U2 = untreated batteries; D1, D2 = batteries with 0.06 wt.% Bi.

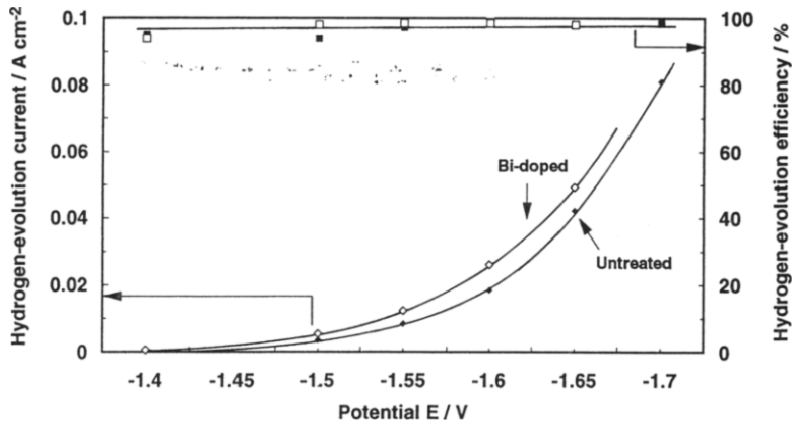

Fig. 9. Hydrogen evolution on pasted electrodes.

(either in the lead used for the manufacture of the oxide and grid alloys, or in the electrolyte) on actual battery performance.

Active material

Only three studies have been found that address the effects of bismuth in the lead from which battery oxide is made. Miyazaki and Sumida [11] found large increases in the cumulative discharge capacity during the deep discharge of batteries produced

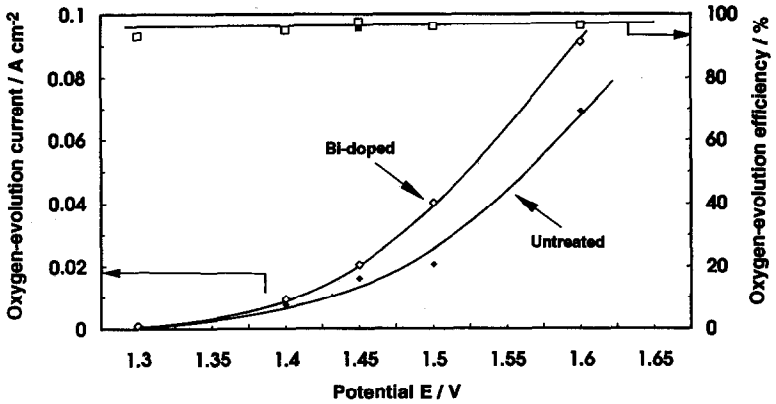

Fig. 10. Oxygen evolution on pasted electrodes.

TABLE 3

Gas pressure peak (kPa) in VRBs during constant-current charging

Cycle number	Untreated batteries		Bi-doped batteries	
	U1	U2	D1	D2
30	13.2	11.2	8.0	11.2
60	13.5	11.0	8.8	4.2
80	16	9.8	11.0	5.9

TABLE 4

Oxygen-recombination efficiency (%) of valve-regulated batteries

Cycle number	Untreated batteries		Bi-doped batteries	
	U1	U2	D1	D2
60	95	93	96	90
80	88	93	86	93
100		90	87	90

either from ball-mill oxide doped with 0.016 wt.% Bi and 0.016 wt.% Tl or from oxide made from lead that contained the same levels of these two dopants. Agruss *et al.* [12] examined the capacity, cycle life, shelf life (28-day test according to SAE specification, 1952) and positive-plate voltage of batteries with bismuth present in the alloy at 0.017 wt.% and in the active material at levels of 0.016, 0.04 and 0.27 wt.%. No significant effects were observed on any of the parameters. In more recent work reported by de Guibert *et al.* [13], battery plates were prepared from leady oxide that was derived from pure lead doped with given amounts of bismuth. Battery tests showed that the presence of bismuth in the oxide at levels up to 0.02 wt.% did not influence the

performance obtained under cycling conditions that simulated automotive service. There was also no significant change in the self-discharge rate, even at a bismuth concentration of 0.043 wt.%.

Electrolyte

Pavlov and co-workers [14, 15] investigated the effect of bismuth on the reconstruction of pulverized active material. The latter was obtained from charged automotive battery plates and was subjected to charge/discharge cycling in tubular electrodes with spines that contained 0 to 0.8 wt.% Bi. Electrodes using spines of pure lead and Pb–6wt.%Sb were also cycled, but in H_2SO_4 solution doped with 0.005 M Bi^{3+}. When present in either the alloy or the electrolyte, bismuth was found to accelerate the establishment of the original active-material skeleton by exerting a catalytic effect on the process of structure restoration. Only 0.2 wt.% Bi was required in the spine alloy to allow the PbO_2 powder to be transformed, after 15 cycles, into a well-organized active material with 50% utilization during discharge. It was also found that bismuth improves the contact between PbO_2 particles and decreases the sensitivity of the plate capacity to the active-mass density. Overall, it was concluded that bismuth exerts a beneficial effect on cycle life, but enhances corrosion at the spine/electrolyte/air boundary.

Maja and Penazzi [10] examined the effect of bismuth on hydrogen evolution and oxygen reduction on charged negative plates at open circuit in a sealed, pressure-sensing, glass vessel. The plates were subjected to a pretreatment of 30 cycles at the 10-h rate in 1.28 sp. gr. H_2SO_4 that contained Bi^{3+} (0.0025 to 0.02 wt.%). After cycling in a solution of 0.01 wt.% Bi^{3+}, plate analysis showed that bismuth had been incorporated into the active material to a level of 0.006 wt.%. Furthermore, the amount of bismuth taken in by the plate was found to increase linearly with the initial bismuth concentration in the electrolyte. Investigations also revealed that bismuth suppressed hydrogen evolution and enhanced oxygen reduction. The extent of this behaviour appeared to be independent of the bismuth concentration. It was claimed that gas recombination in VRBs could be improved by the presence of bismuth.

Grid alloys

Devitt and Myers [16] examined the cycle life of batteries produced from lead–calcium–tin grids that contained 0.0007 to 0.042 wt.% Bi. Two cycling regimes were applied, namely, the SAE J537 and SAE J240 procedures. The results revealed no effect of bismuth on cycle life and gassing/corrosion rates for batteries subjected to the SAE J537 regime. By contrast, an increasing bismuth content produced an enhancement in the cycle life of batteries under the SAE J240 test. Masanobu *et al.* [17] subjected batteries using Pb–1.5wt.%Sb grids with 0 to 0.15 wt.% Bi to the JIS D5301 procedure. It was found that the optimum performance was obtained by the addition of 0.05 wt.% Bi to the grid alloy. Similar tests were conducted by Takahide and Hiroshi [18] on batteries with Pb–1.5wt.%Sb grids that contained 0 to 0.3 wt.% Bi. The best cycle lives were observed for batteries produced from grids with 0.1 and 0.2 wt.% Bi. Gibson *et al.* [19] found that bismuth levels of up to 0.26 wt.% in lead–calcium–tin alloys gave no effect on 20-h discharge capacity, reserve capacity, self discharge, and deep cycling. Hoehne [20] studied the performance of batteries constructed either with Pb–5.5wt.%Sb grids containing 0.006 to 0.23 wt.% Bi or with pure-lead Planté plates containing 0.006 to 0.205 wt.% Bi. The work showed that bismuth exerted little influence on the cycle life of the antimonial batteries, but promoted the shedding of positive active material and increased the growth of grids in Planté plates.

Model alloy systems

A large body of research has been devoted to understanding the effects of bismuth in lead alloys, especially in lead–bismuth binary systems. These alloys have been examined as bare (i.e., unpasted) 'model' electrodes. The major findings have recently been reviewed in detail by Koop *et al.* [21]. This survey revealed that the experimental results are both complex and often contradictionary. Furthermore, it would appear that most of the alloys tested to date are not relevant to either conventional or valve-regulated battery systems.

Conclusions

In the studies reported here, the important observations are that the inclusion of bismuth at levels up to 0.06 wt.% in both the positive and the negative active materials causes no significant differences in the cycle life of automotive batteries that use low-antimony grid alloys, but enhances the capacity/cycle life and lowers the gas evolution of VRBs. The benefits of bismuth observed both in this study and by the other researchers, together with confirmation of the absence of any ill-effects, will encourage a minimum bismuth content to be set in the specification for lead that is used in the production of leady oxide. Although the present results have shown significant advantages in having 0.06 wt.% Bi in the active material, and optimum level has yet to be determined. This is a prime target of the on-going collaborative research programme between Pasminco and CSIRO.

Acknowledgements

The authors are grateful to their colleagues, J.F. Kelly and L. Cranswick, for early experimental in the project, Hammond Lead Products Inc. for the supply of leady oxides, and GNB Australia Ltd. for the construction of batteries.

References

1 L.T. Lam, J.D. Douglas, R. Pillig and D.A.J. Rand, *J. Power Sources, 48* (1994) 219.
2 N.D. Hung, J. Garche and K. Wiesener, *Tap Chi Hoat Dong Khoa Hoc, 26* (1988) 8.
3 N.D. Hung, J. Garche and K. Wiesener, *Tap Chi Hoat Dong Khoa Hoc, 27* (1989) 1.
4 H. Dietz, S. Voss, H. Doring, J. Garche and K. Wiesener, *J. Power Sources, 31* (1990) 107.
5 H. Dietz, M. Radwan, J. Garche, H. Doring and K. Wiesener, *J. Appl. Electrochem., 21* (1991) 221.
6 D. Pavlov and G. Papazov, *J. Appl. Electrochem., 6* (1976) 339.
7 L.T. Lam, R. De Marco, J.D. Douglas, R. Pillig and D.A.J. Rand, to be published.
8 E.A. Khomskaya, N.F. Gorbacheva and N.B. Tolochkov, *Electrokhimiya, 16* (1980) 48.
9 C.S.C. Bose and N.A. Hampson, *B. Electrochem., 4* (1988) 437.
10 M. Maja and N. Penazzi, *J. Power Sources, 22* (1988) 1.
11 K. Miyazaki and M. Sumida, in K.R. Bullock and D. Pavlov (eds.), *Proc. Symp. Advances in Lead-Acid Batteries,* Proc. Vol. 84-14, The Electrochemical Society, Pennington, NJ, USA, 1984, p. 78.
12 B. Agruss, E.H. Herrmann and F.B. Finan, *J. Electrochem. Soc., 104* (1957) 204.
13 A. de Guibert, B. Chaumont, L. Albert, J.L. Caillerie, A. Ueberschaer, R. Höhn, W. Davis and M.J. Weighall, *J. Power Sources, 42* (1992) 11.

14 D. Pavlov, *J. Power Sources, 33* (1991) 221.
15 D. Pavlov, A. Dakhouche and T. Rogachev, *J. Power Sources, 30* (1990) 117.
16 J.L. Devitt and M. Myers, *J. Electrochem. Soc., 123* (1976) 1769.
17 S. Masanobu, N. Hiroto, A. Masahiro and K. Hiroshi, *Jpn. Patent No. 61 203 568* (1986).
18 N. Takahide and F. Hiroshi, *Jpn. Patent No. 6 319 768* (1988).
19 I.K. Gibson, K. Peter and F. Wilson, in J. Thompson (ed.), *Power Source 8, Research and Development in Non-mechanical Electrical Power Sources,* Academic Press, London, 1981, p. 565.
20 E. Hoehne, *Metallwirtsch., 23* (1944) 60.
21 M.J. Koop, D.A.J. Rand and B. Culpin, *J. Power Sources, 45* (1993) 365.